PORTLAND
PRESS

Review Article

A case for low atmospheric oxygen levels during Earth's middle history

Noah J. Planavsky[1,2], **Devon B. Cole**[1], **Terry T. Isson**[1], **Christopher T. Reinhard**[2,3], **Peter W. Crockford**[4,5], **Nathan D. Sheldon**[6] and **Timothy W. Lyons**[2,7]

[1]Department of Geology and Geophysics, Yale University, New Haven, CT, U.S.A.; [2]NASA Astrobiology Institute Alternative Earths Team, Riverside, CA, U.S.A.; [3]School of Earth & Atmospheric Sciences, Georgia Institute of Technology, Atlanta, GA, U.S.A.; [4]Department of Earth and Planetary Sciences, Weizmann Institute of Science, Rehovot 76100, Israel; [5]Department of Geosciences, Princeton University, Princeton, NJ 08544, U.S.A.; [6]Department of Earth and Environmental Sciences, University of Michigan, Ann Arbor, MI, U.S.A.; [7]Department of Earth Sciences, University of California, Riverside, CA, U.S.A.

Correspondence: Noah J. Planavsky (noah.planavsky@yale.edu)

The oxygenation of the atmosphere — one of the most fundamental transformations in Earth's history — dramatically altered the chemical composition of the oceans and provides a compelling example of how life can reshape planetary surface environments. Furthermore, it is commonly proposed that surface oxygen levels played a key role in controlling the timing and tempo of the origin and early diversification of animals. Although oxygen levels were likely more dynamic than previously imagined, we make a case here that emerging records provide evidence for low atmospheric oxygen levels for the majority of Earth's history. Specifically, we review records and present a conceptual framework that suggest that background oxygen levels were below 1% of the present atmospheric level during the billon years leading up to the diversification of early animals. Evidence for low background oxygen levels through much of the Proterozoic bolsters the case that environmental conditions were a critical factor in controlling the structure of ecosystems through Earth's history.

Why the mid-Proterozoic?

Over the past decade, there has been a surge of work reconstructing Earth's oxygenation. This work has been largely fueled by the desire to reconstruct the role of environmental factors in driving broad-scale evolutionary trends [1–5]. Foremost, there has been extensive debate about whether the late appearance and diversification of animals were linked to a change in environmental oxygen levels, or whether this major shift in the structure and complexity of the biosphere simply reflects the timing of genetic innovation and ecosystem restructuring independent of any environmental control. Historically, estimates of mid-Proterozoic (1.8–0.8 Ga) atmospheric oxygen levels [6] have ranged widely. Within this range, higher estimates of Proterozoic surface oxygen levels suggest the timing of the rise of animals was probably decoupled from environmental controls (i.e. habitable oxygenated environments substantially preceded the appearance of animals), whereas lower Proterozoic pO_2 estimates suggest a late rise in atmospheric oxygen, implicating environmental exclusion of animals for the majority of Earth's history.

Furthermore, as we develop tools to characterize the atmospheric composition of planets beyond our solar system, there has been increased focus on determining how Earth would appear if analyzed remotely over its history [7,8]. The presence of strong atmospheric redox disequilibria (e.g. oxygen and methane) is classically one of the strongest candidates for a robust, remotely detectable biosignature [9]. There is locally detectable evidence for extensive life on Earth for at least the last 3.5 billon years [10]; however, there is no clear consensus regarding the record of atmospheric redox disequilibria. There are only poor constraints on atmospheric methane concentrations through Earth's history, but much of our uncertainty about the history of redox disequilibria through Earth's history lies with

1

imprecise pO_2 estimates [8]. Not surprisingly, there is also debate about the processes controlling atmospheric oxygen levels. In summary, there are several critical questions about biotic and environmental co-evolution that cannot be answered without tackling the history of atmospheric oxygen on our planet.

Partly due to revolutionary insights into Archean atmospheric chemistry [∼3.8–2.5 billion years ago (Ga)] afforded by developments in the rare sulfur (S) isotope system (e.g. [11–13] and many others), atmospheric O_2 during Proterozoic time (∼2.5–0.54 Ga) remain perhaps the most enigmatic in Earth's history (see [3,6]). Archean atmospheric pO_2 were predominantly well below ∼10^{-5} times the present atmospheric level (PAL) [13], while the charcoal record strongly suggests that pO_2 values during most of the last ∼400 million years have been above ∼50% PAL (e.g. [14–16]). However, mid-Proterozoic (1.8–0.8 Ga) pO_2 values have previously been only broadly constrained to be ∼1–40% PAL [6] and are conventionally assumed to be ∼10% PAL [6]. The lower limit of this range is traditionally diagnosed based on the retention of Fe^{3+} in Proterozoic paleosols, while the upper limit is constrained by ventilation dynamics of a simple three-box ocean model [17]. Here, rather than focus on potential ramifications of different oxygen reconstructions [2,3,5], we explore the lines of evidence that point toward predominantly low (<1% PAL) mid-Proterozoic atmospheric oxygen levels and consider factors that could have led to this Earth system state.

Tools to track Proterozoic oxygen levels

Lower estimates of atmospheric composition for the Proterozoic have most commonly come from the major element composition of lithified soil profiles (paleosols). These estimates are generally derived from either 'steady-state' or 'kinetic' techniques. Steady-state techniques (e.g. [18,19]) compare the relative oxidant (D_{O_2}) and acid (D_{CO_2}) demand of a parent material via expressions of the form (eqn 1):

$$R = \frac{D_{O_2}}{D_{CO_2}} \sim \frac{0.25m_{FeO} + 0.5m_{MnO}}{2[m_{CaO} + m_{MgO} + m_{Na_2O} + m_{K_2O} + m_{CaMg(CO_3)_2}]},$$

where m_i values are concentrations (mol kg^{-1} of rock). For a given parent rock, D_{O_2} represents the O_2 required to oxidize Fe^{2+} and Mn^{2+} quantitatively, and D_{CO_2} represents the carbonic acid needed to remove all Ca, Mg, Na, and K phases. In principle, this ratio can be related to the ambient partial pressures of CO_2 and O_2 during weathering by assuming that the soil profile has reached steady state.

Despite problems associated with accurate corrections for the retention of Ca, Mg, and Na phases in paleosols and introduction of K during metasomatism and limitations associated with assuming steady state [19], this approach has the advantage of greatly minimizing the free parameters required to estimate the atmospheric O_2/CO_2 ratio for a given weathering system. However, a notable drawback is that estimating O_2 (or CO_2) requires the assumption of a value for CO_2 (or O_2), neither of which is typically well constrained. Subsequently, Sheldon [20] developed an alternative method based on an integrated mass balance approach that does not require assumption of a pO_2 value to invert paleosol observations for pCO_2 (or vice versa). Instead, this approach requires explicit specification of an infiltration (rainfall) rate and depth of the water table (discussed in detail in [20,21]) — in most cases requiring use of a decompaction algorithm [22] to reconstruct original sample soil profile depths. This mass balance approach yields estimates that are consistent with extremely low atmospheric pO_2 values (Figure 1), despite being frequently leveraged to suggest a firm constraint on pO_2 of >1% PAL for much of Proterozoic time [6]. Furthermore, although mid-Proterozoic paleosols were originally proposed to be characterized by complete Fe oxidation, more recent work suggests that the most straightforward examples of paleosols from this time are actually characterized by Fe loss rather than Fe retention relative to the pre-weathering composition of the parent material (Figure 2) [23–25]. Early paleosol work did not consider volume change during soil formation, in some cases providing false signals for iron retention. Furthermore, the classic 1.1 Ga Sturgeon Falls paleosol studied by Dick Holland, which was reported as evidence of complete Fe retention, turned out, in a follow-up study, to be a combination of felsic and mafic material rather than developing from bedrock [23–25]. As such, the most commonly cited estimate for lower oxygen across the mid-Proterozoic is built from an outdated view of paleosols. A new update of the paleosol record through time is needed. However, given the standard framework, mid-Proterozoic paleosols should be viewed as providing a maximum rather than a minimum constraint on pO_2 of ∼1% PAL.

Chromium isotopes have emerged in recent years as an alternative window to ancient pO_2 (e.g. [4,26–29]). This system is grounded in the idea that variability in $\delta^{53}Cr$ in the sedimentary rock record requires the
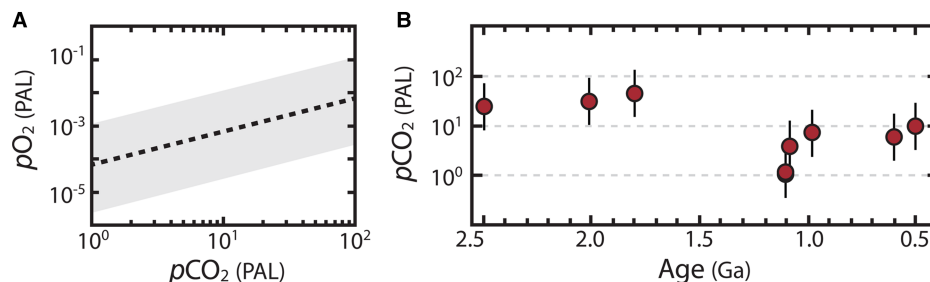
Figure 1. Paleosol constraints on atmospheric composition during mid-Proterozoic time.
Shown in (**A**) are calculated pO_2 values as a function of assumed pCO_2 values using the estimated R value (and associated error) for the Sturgeon Falls paleosol (~1.1 Ga) from ref. [19]. Shown in (**B**) are reconstructed pCO_2 values (and estimated error) based on the integrated mass balance approach [20,70]; the value for pCO_2 at 0.6 Ga is a new calculation based on data published by Liivamagi et al. [71] assuming a formation time of 1 Myr.

formation and transport of mobile Cr(VI) in surface environments and that the formation of this species requires free oxygen [28]. Oxidized and mobile Cr(VI) is isotopically enriched, whereas mobile Cr(III) is largely unfractionated relative to igneous values. Within this framework, limited variability in the δ^{53}Cr sedimentary record is indicative of oxygen levels below those required for oxidative Cr cycling, while the onset of variability in the δ^{53}Cr record should mark a shift to oxidative terrestrial weathering of Cr and, more broadly, oxidized surface environments. Chromium oxidation is typically thought to be inhibited in marine environments because of the sparing solubility of Cr(III) at circumneutral pH — a key component of the rationale behind using Cr as an O_2 paleobarometer [28].

The Cr isotope proxy can be coupled — as in paleosol studies — to quantitative weathering models. Two main approaches have been used to approximate the surface oxygen levels needed to induce Cr isotope fractionations: (1) estimating the levels of oxygen needed to induce extensive Cr(III) oxidation and (2) estimating the
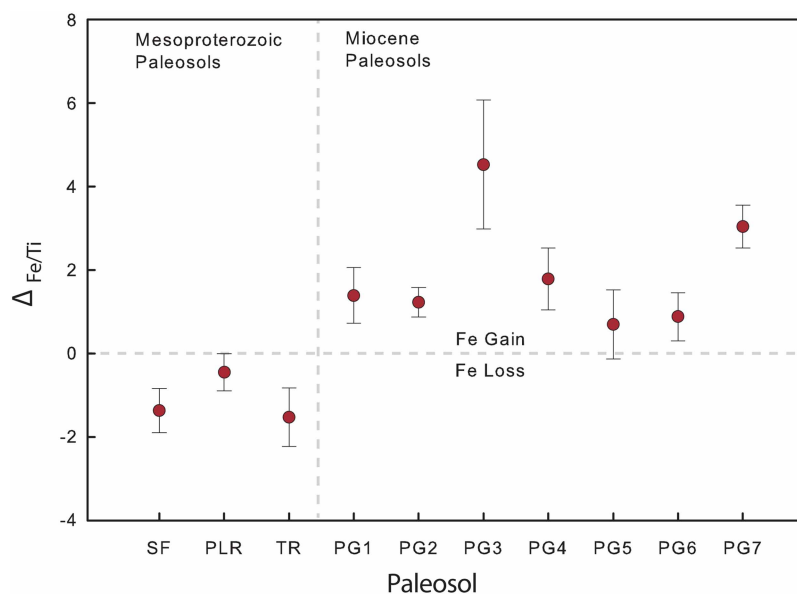

Figure 2. Fe retention for basalt-protolith Mesoproterozoic and Miocene paleosols.
Retention or loss of Fe is calculated as $\Delta_{Fe/Ti} = (Fe/Ti)_{paleosol} - (Fe/Ti)_{parent}$, where Fe is total Fe as Fe^{3+} and Ti is considered an immobile element during weathering. Whereas Miocene-aged paleosols have all retained or gained Fe during pedogenesis relative to the parental basalt, all of the Mesoproterozoic paleosols have lost a significant amount of Fe relative to their parent materials. SF, sturgeon falls [19,24]; PLR, pike lake road; TR, temperance river (both TR and PLR are from [70]); PG1–7, Picture Gorge Subgroup paleosols from the Columbia River Basalt Province [72].

levels of oxygen needed to oxidize Fe(II) quantitatively in the weathering environment. The former relies on kinetic data from modern settings and the observation that Cr oxidation typically proceeds via Cr(III) surface interaction with solid-phase Mn oxides [30]. Therefore, with this approach, the key oxygen-dependent process is terrestrial Mn oxidation. One major uncertainty in this approach is fluid residence time in soils — a common problem for kinetic weathering models. Nevertheless, using this approach, significant coupled Mn–Cr oxidation should take place at or below ~0.1% PAL [4].

Using the approach described above, soil Fe oxidation can also be linked to Cr cycling and associated isotope variability, given that Fe(II) is a potent reductant for Cr(VI). If Fe(II) is present in the upper part of the weathering system, transport of Cr(VI) out of the soils and subsequent Cr isotope variability in surface waters will be inhibited. As outlined above, there are uncertainties in modeling the amount of oxygen required to quantitatively oxidize Fe(II) in typical weathering environments, but most estimates range between ~0.1 and 1% PAL.

Initial attempts to reconstruct Earth's atmospheric oxygenation from Cr isotope analysis relied on banded iron formations [28] and ironstones [4], which provided evidence for abundant mobile but unfractionated Cr in the early and middle Proterozoic (Figure 3). Iron formations and ironstones were targeted because they consist largely of primary precipitated phases and are therefore likely to develop large authigenic (seawater-derived) Cr enrichments. Large Cr enrichments also increase the chances that these sediments will be highly rock-buffered and thus resistant to later diagenetic influence.

Recently, researchers have explored other sedimentary archives with the potential to record shifts in the δ^{53}Cr record, including relatively ubiquitous organic-rich black shales and carbonate rocks (limestones and dolostones) (Figure 3). Muds have been shown to capture modern marine variability in δ^{53}Cr values in the recent sedimentary record (e.g. [31]). This archive has subsequently been expanded into deep time and provides evidence for the onset of oxidative Cr cycling at ~800 Ma, coincident with independent evidence for eukaryotic diversification [26]. In contrast, Gilleaudeau et al. [29] reported both unfractionated and fractionated δ^{53}Cr values from bulk carbonate analyses at ~1.1 Ga. If primary, this observation suggests oxygen levels above ~0.1–1% PAL by the late Mesoproterozoic. Carbonate rocks, however, are particularly susceptible to diagenetic alteration, commonly experiencing pervasive recrystallization, and trace metal signatures in carbonates are commonly diagenetic in origin, including overprinting from later diagenetic fluids (e.g. [32]). Furthermore, experimental work suggests that moderate fractionations (~0.3‰) are possible during incorporation of Cr(VI) during carbonate precipitation [33], but there has not yet been a systematic investigation of Cr(III) incorporation and fractionations associated with this process.

Several complications with the basic Cr isotope framework have emerged since the proxy was first introduced as a tool for tracking atmospheric oxygenation. For example, there is compelling evidence that environmental Mn oxidation commonly proceeds via superoxide formation (e.g. [34]). Although still ultimately tied to O_2, this process complicates modeling the kinetics of Cr oxidation. Furthermore, high-temperature serpentinization, in the absence of O_2, can lead to strong Cr isotope fractionations and a mobile, isotopically fractionated Cr reservoir (e.g. [35,36]), while other evidence suggests that Cr(III) complexation with organic acids and ligands can also lead to large δ^{53}Cr fractionations [37]. Despite these complications, we suggest that the basic qualitative framework for using Cr isotopes as a paleoredox proxy need only be modified rather than abandoned. In particular, the common occurrence of mobile but unfractionated Cr [26,28] suggests that Cr(III) moving through Earth's surface is not ubiquitously affected by organic complexation or serpentinization and will always be a spatially restricted process. Therefore, a pronounced change in average sedimentary δ^{53}Cr values is still likely to be linked to shifts in surface oxygen levels.

In summary, we suggest that the shift to consistently fractionated Cr isotope values in the sedimentary record of shales and iron-rich chemical sediments is a robust signal for the onset of a predominantly oxidative Cr cycle at ~800 Ma. However, the Cr isotope record does not preclude the possibility of ephemeral swings to higher pO$_2$ levels for some intervals earlier in the Proterozoic. Future research should focus on improving our understanding of surface Cr cycling in modern environments and the diagenetic history of the various potential sedimentary archives. Additional work is also required to tighten constraints on oxidation kinetics under conditions pertinent to natural weathering environments and to improve the range of quantitative models employed to explain Cr isotope records. Nevertheless, the first-order trends in the sedimentary Cr isotope record are striking and suggest low (<1% PAL) background pO$_2$ levels through the mid-Proterozoic.

Triple oxygen isotopes are another emerging system that may provide powerful quantitative insights into Earth's atmospheric evolution. This system capitalizes on anomalous enrichments or depletions in the rare ^{17}O isotope relative to the relationship expected for a purely mass-dependent process — so-called mass-independent
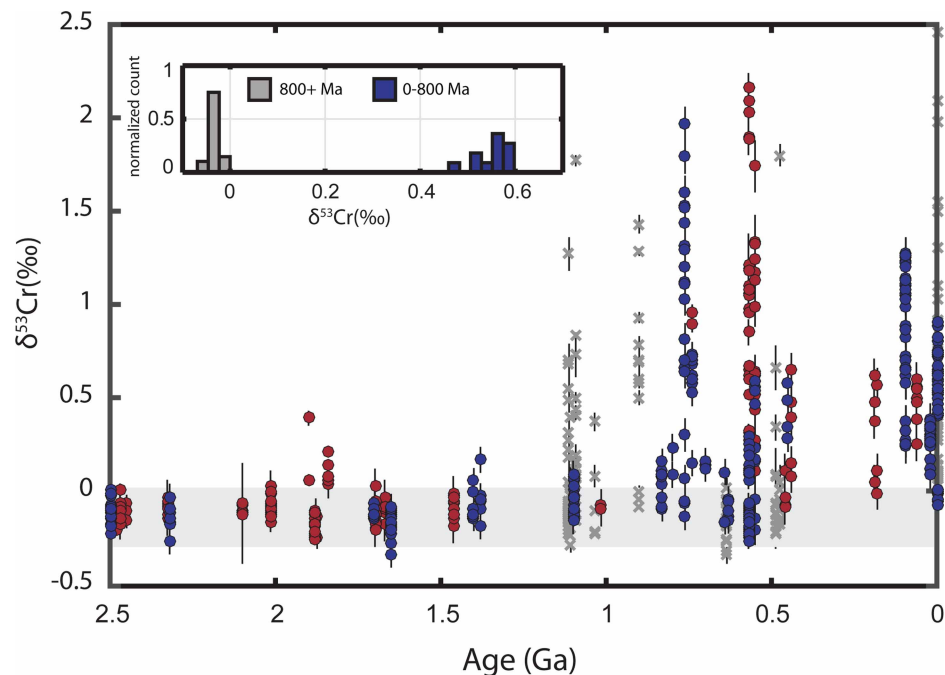
Figure 3. Compiled marine sedimentary Proterozoic and Phanerozoic Cr isotope record. Ironstones and iron formations in red, shales in blue, and carbonates in gray. Inset shows bootstrap resampled mean distributions of early and mid-Proterozoic (gray) and late Proterozoic and Phanerozoic (blue) Cr isotope data from all sedimentary archives [4,26–29].

fractionations (MIF) or non-mass-dependent isotope effects. The first of these MIF isotope effects was observed in laboratory experiments examining ozone (O_3) formation [38]. These experiments revealed that the symmetry of the excited O_3 molecule following collision between O atoms and O_2 in the Chapman cycle controls whether it will relax to a ground-state O_3 molecule or dissociate back into O and O_2. The result is that O_3 formed in the stratosphere is, relative to the expectations of a purely mass-dependent process, anomalously enriched in the 'rare' ^{17}O isotope (denoted as a positive $\Delta^{17}O$ value) [39]. This positive $\Delta^{17}O$ signal is trans-ferred via the single O photolysis product to CO_2 [40], while the complementary negative $\Delta^{17}O$ signal is stored in residual stratospheric O_2. Critically, such reactions can only occur at a sufficient atmospheric O_2 level to ini-tiate stratospheric photochemical reaction networks. Previous estimates have placed this threshold at ∼0.1% PAL [41], which provides an important minimum pO_2 constraint for sediments bearing $\Delta^{17}O$ anomalies.

Isotopically anomalous O_2 is mixed down into the troposphere, consumed by aerobic respiration, and replaced by isotopically 'normal' O_2 produced from photosynthesis (e.g. [42]). As a result, the $\Delta^{17}O$ value of O_2 in the troposphere reflects the mass balance between sourcing of anomalous O_2 from photochemistry in the stratosphere (the magnitude of which varies with the size of the atmospheric CO_2 and O_2 reservoirs) and the gross oxygen flux from the biosphere. This $\Delta^{17}O$ anomaly in tropospheric O_2 can be transferred to dis-solved SO_4^{2-} in surface waters during the oxidative weathering of pyrite and preserved over geologic time in sedimentary sulfate minerals (e.g. [43]). Building from this framework, there are three principal factors that will control the $\Delta^{17}O$ composition of tropospheric O_2 at any given time: (1) atmospheric O_2 levels, (2) atmos-pheric CO_2 levels, and (3) the gross oxygen flux of the biosphere, which has been used as an approximation for primary production [often thought of as gross primary productivity although one could make an argument that net primary productivity (NPP) is the more appropriate flux, see refs [44–46] and references therein].

Crockford et al. [45] recently found the first evidence of anomalously negative $\Delta^{17}O$ values outside of those linked to Snowball Earth events — with values low as −0.9‰ [45] — in terrestrial sulfates from the ∼1.4 Ga Sibley Group. Many of the parameters necessary to translate these sulfate oxygen isotope values to either primary productivity or pO_2 estimates, as discussed above, are only roughly constrained for the mid-Proterozoic. As such, there are multiple non-unique combinations of pO_2–pCO_2-primary productivity that can lead to a single sedimentary $\Delta^{17}O$ value [45]. However, the magnitudes of the biospheric flux of O_2 and pO_2 are directly coupled and there are rough estimates of mid-Proterozoic pCO_2. Therefore, only a

fraction of the mathematically possible pO_2–pCO_2-primary productivity combinations that can produce strongly negative $\Delta^{17}O$ values are actually biogeochemically feasible solutions for a stable mid-Proterozoic Earth system [45].

We have revisited the range of pO_2–pCO_2-primary productivity combinations that can generate anomalously negative $\Delta^{17}O$ values under stable Earth system states (see also ref. [45]), assuming an intimate link between atmospheric O_2 levels and NPP. Despite the potential for deviations in the reductant flux to Earth's surface through time, it has been recently argued that there is a relatively limited range of organic burial rates that can result in a stable Proterozoic oxygen state (assuming pO_2 estimates ranging from 0.1to 10% PAL) [e.g., 47,48]. This idea stems, in part, from a global biogeochemical model that has a set of generally accepted oxygen cycle feedbacks (e.g. enhanced organic carbon burial under anoxic marine conditions) [48]. To build from the Laakso and Schrag [47,48] models, we sought to define a range of reasonable organic matter burial efficiencies in mid-Proterozoic ocean — which are generally accepted to be largely anoxic and have low sulfate levels relative to the modern — using a simple reaction transport model that tracks organic matter remineralization during passage through the water and sediment column (Figure 4). We used an organic degradation rate law based on empirical observations in modern low sulfate systems [49] and assumed a range of settling times (see Table 1 for parameter ranges). Using this approach, we estimate that organic carbon burial efficiencies for the mid-Proterozoic were between ~10 and 32% (Figure 4). With this range of burial efficiencies coupled to model-based estimates of mid-Proterozoic organic carbon burial [47], it is possible to define a reasonable range for primary productivity and subsequently use the Sibley Group $\Delta^{17}O$ values to estimate mid-Proterozoic atmospheric composition (see also ref. [45]).

The final step to translate the Sibley Group oxygen isotope data into atmospheric oxygen estimates after considering assumptions about the links between primary productivity and pO_2 is to systematically consider the uncertainties in other key parameters that affect sedimentary $\Delta^{17}O$ values. Following Crockford et al. [45], we translate $\Delta^{17}O$ into pO_2–pCO_2-primary productivity combinations using a Monto Carlo simulation (see ref. [45] for simulation details; Figure 4). For this simulation, we use the Laakso and Schrag [47] Proterozoic organic carbon burial estimates (and assume 100% error), Proterozoic terrestrial oxygen flux estimates (ref. [50]; G3 scenario), organic burial efficiency between 10 and 32%, possible pCO_2 values between 2 and 100 times preindustrial atmospheric levels (280 ppm CO_2: PIAL), and confined pO_2 solutions to vary between 0.1 and 10% PAL. This assumed pO_2 range covers recently proposed, low, mid, and upper Proterozoic atmospheric oxygen estimates (e.g. [26,29,51–54]). With these forcings and the new Sibley $\Delta^{17}O$ values, we estimate that primary productivity was less than 3% of modern levels and that mid-Proterozoic pO_2 values were between 0.1 and 1.75% PAL. Assuming a mean organic carbon burial efficiency of 25%, which is close to our average estimated burial efficiency (Figure 4), pO_2 estimates are <1% PAL (Figure 4). These pO_2 estimates are consistent with contemporaneous paleosol and Cr isotope records (see above). The $\Delta^{17}O$ system is complicated, and this exercise should, by no means, be viewed as the final attempt at revisiting the significance of the Sibley Group $\Delta^{17}O$ data [45]. Regardless, the recent discovery that sedimentary mid-Proterozoic $\Delta^{17}O$ values are anomalous relative to the Phanerozoic record provides a tantalizing additional line of evidence that atmospheric oxygen levels during Earth's middle history were were distinct — dramatically lower than those of the modern Earth, as well as dramatically higher than those of the Archean.

Surface- and deep-marine redox conditions have been used extensively in attempts to track atmospheric oxygenation (e.g. [1,17,55]). The basic premise behind this approach is straightforward — gases in surface waters are often close to equilibrium with the atmosphere, and the amount of oxygen in downwelling water masses is a primary factor controlling oxygen levels in the deep sea. There are numerous records of expansive anoxia in the Proterozoic and even some for shallow water anoxia (e.g. [3,56–59]) — generally consistent with low Proterozoic atmospheric oxygen levels. However, it should also be noted that there are short-lived intervals of widespread anoxia in the Phanerozoic — potentially even within the mixed layer — when atmospheric oxygen levels were near modern levels (e.g. [60]). It is generally accepted that deep-ocean oxygenation occurred at the end of the Proterozoic or in the Phanerozoic [3,51,56–58,59]. Nonetheless, there are also reports of Proterozoic oxic/suboxic deepwaters [53,61,62], which, at first blush, paint a different picture of surface oxygen levels. However, coupling marine redox proxies to atmospheric oxygen levels is not necessarily straightforward. With lower atmospheric oxygen levels (e.g. less than ~5% PAL), surface waters are expected to be highly variable and far from equilibrium [63], complicating our ability to directly link marine oxygen levels to atmospheric composition. In addition, deep-marine oxygen levels are also strongly controlled by the strength of the biological pump, and to some extent the biological pump must be coupled to pO_2 (e.g. [47,50,64]) which, as outlined
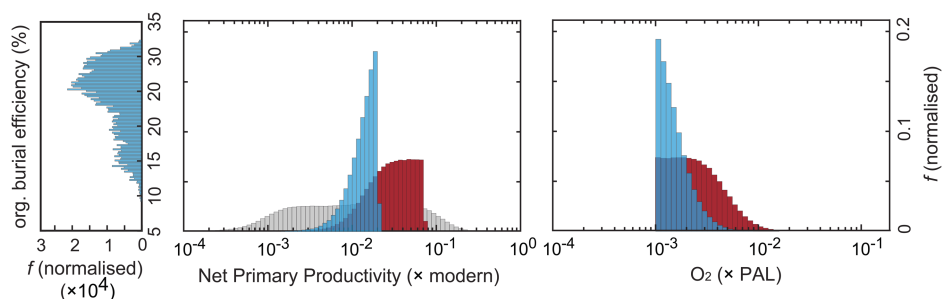
Figure 4. A statistical approach to using sulfate $\Delta^{17}O$ values to track Proterozoic atmospheric oxygen levels.
Sulfate mineral $\Delta^{17}O$ signatures vary as a function of atmospheric O_2 and CO_2, and NPP. However, O_2 and NPP are intimately linked via organic carbon burial, and mid-Proterozoic CO_2 values are likely to have been between 2 and 100 PIAL [20,70], making it possible to use $\Delta^{17}O$ data to estimate a range of atmospheric oxygen levels. (left pannel) Estimated marine organic burial efficiency (%) for predominantly anoxic oceans using the organic degradation rate laws in ref. [49]. (central and right panels) Monte Carlo solutions for primary productivity and O_2 based on the $\Delta^{17}O$ values from the 1.4 Ga Sibley Group [45] and parameters listed in Table 1. f denotes the normalized frequency of the analysis. Primary productivity and O_2 results are filtered according to possible stable oxygen states in ref. [47] — using organic burial efficiencies of 1% (red) and 25% (blue). Gray bars show the possible range of NPP without filtering for reasonable coupling between NPP and pO_2.

above, was likely dramatically different in the mid-Proterozoic than in the modern. Thus, caution is required when linking the marine redox landscape to atmospheric oxygen levels.

A low oxygen earth system

Multiple proxy records suggest a generally low oxygen state through the mid-Proterozoic, which requires a set of global biogeochemical conditions dramatically different from those operating today. It has been argued that limited primary productivity and low rates of organic carbon burial, relative to the modern, are essential for low (<1% PAL) atmospheric oxygen levels, given a reasonable possible range of reductant fluxes (e.g. [47,48]). The most obvious mechanism for dramatically reducing primary productivity is to reduce the amount of nutrients available for oxygenic photosynthesizers (e.g. [64]). Phosphorus is typically regarded as the ultimate limiting nutrient (e.g. [64]), and there is some empirical support for persistent, severe P limitation throughout most of the Precambrian [65]. Critically, there are several scenarios whereby a largely anoxic ocean — a consequence of low atmospheric pO_2 — would be expected to trigger a nutrient crisis [64–66]. Foremost, there is likely to be enhanced abiogenic P scavenging in an anoxic ocean [64–66]. Although it has been argued that P may be inefficiently buried in euxinic settings (anoxic and sulfidic) (e.g. [67]), sulfidic waters were likely not the dominant reducing environment for the majority of the Proterozoic [59].

Table 1 $\Delta^{17}O$ model parameters

	Parameter value	References
Oxic layer thickness (m)	200	—
Organic sinking rate (m day^{-1})	0.6–4	Bach et al. [73]
Sedimentation rate (cm day^{-1})	Shelf 0.3–0.4; Slope 0.05–0.2; Open Ocean 0.003–0.01	Thullner et al. [74]
Proportion of sea floor (%)	Shelf 7; Slope 11; Open Ocean 82	Thullner et al. [74]
Modern global NPP (Tmol C yr^{-1})	8000	Woodward [75]
Proterozoic marine NPP (Tmol C yr^{-1})	43 (for 10% burial eff) 13 (for 32% burial eff)	This study
CO_2 range (PIAL)	2–100	Sheldon [70]
O_2 range (% PAL)	0.1–10	Crockford et al. [45]

With lower amounts of oxygen released from photosynthesis because of lower amounts of organic carbon burial during the mid-Proterozoic, it would have been possible to consume the majority of biologically produced oxygen through reaction with volcanic gases and through ferrous iron oxidation within the terrestrial realm. Given that the kinetics of these reactions are extremely rapid [68] — relative to the main oxygen consumption pathway in modern terrestrial systems (organic carbon oxidation) — low atmospheric oxygen levels would have been sustained (see also ref. [69]). The Archean can be thought of as an Earth system state during which reduced gas fluxes (e.g. H_2, SO_2, and CH_4) were greater than biological oxygen fluxes. This situation would have led to the accumulation of excess reductant in the atmosphere. In contrast, in the mid-Proterozoic Earth system state, biological oxygen fluxes must have been higher than volcanic reduced gas fluxes — but not high enough to fully oxidize the terrestrial weathering realm. The atmosphere would have been oxidizing (e.g. $O_2 \gg CH_4$), but low oxygen levels would have been maintained, given rapid consumption of oxygen via partial iron oxidation within soils. Critically, the paleosol and Cr isotope records provide direct evidence for this mode of atmospheric oxygen regulation (e.g. partial iron oxidation in the terrestrial realm). In contrast, in the modern well-oxygenated Earth system state, extensive organic carbon oxidation (including through fires) sets a maximum limit on atmospheric oxygen levels [14].

Conclusions and future directions

Multiple traditional and 'novel' atmospheric redox proxies point to low (<1% PAL) atmospheric oxygen levels for much of the mid-Proterozoic. This evidence must be part of any discussion regarding the role of oxygenation in the delayed rise of animals to ecological prominence. A critical next step will be grappling with how to incorporate these environmental constraints into quantitative ecological models and phylogenetic frameworks. However, despite new records and constraints on Earth's oxygenation that have emerged over the past decade, there is much work to be done. Current records remain sparse, and our view of the mid-Proterozoic Earth is painted with only broad strokes. There are hints of a more complex and dynamic oxygenation history than the traditionally imagined unidirectional rise — but this should not be surprising. In fact, with lower atmospheric oxygen conditions and a smaller oxygen reservoir to buffer redox imbalances, dramatic swings in surface oxygen levels should be expected, even with feedbacks stabilizing the Earth system in a low oxygen state. Nonetheless, we feel a strong case can be made for low (<1% PAL) background atmospheric oxygen levels through most of Earth's history and look forward to future work and challenges designed to test this model and its implications.

Summary

- Multiple traditional and 'novel' atmospheric redox proxies point to low (<1% PAL) atmospheric oxygen levels for much of the mid-Proterozoic.

- Evidence for low atmospheric oxygen levels in the mid-Proterozoic should be part of the discussion on the factors leading to the delayed rise of animals to ecological prominence.

PORTLAND
PRESS

References

1   Canfield, D.E., Poulton, S.W. and Narbonne, G.M. (2007) Late-Neoproterozoic deep-ocean oxygenation and the rise of animal life. *Science* **315**, 92–95 https://doi.org/10.1126/science.1135013

2   Lenton, T.M., Boyle, R.A., Poulton, S.W., Shields-Zhou, G.A. and Butterfield, N.J. (2014) Co-evolution of eukaryotes and ocean oxygenation in the Neoproterozoic era. *Nat. Geosci.* **7**, 257–265 https://doi.org/10.1038/ngeo2108

3   Lyons, T.W., Reinhard, C.T. and Planavsky, N.J. (2014) The rise of oxygen in Earth's early ocean and atmosphere. *Nature* **506**, 307–315 https://doi.org/10.1038/nature13068

4   Planavsky, N.J., Reinhard, C.T., Wang, X., Thomson, D., McGoldrick, P., Rainbird, R.H. et al. (2014) Low mid-Proterozoic atmospheric oxygen levels and the delayed rise of animals. *Science* **346**, 635–638 https://doi.org/10.1126/science.1258410

5   Sperling, E.A., Knoll, A.H. and Girguis, P.R. (2015) The ecological physiology of Earth's second oxygen revolution. *Annu. Rev. Ecol. Evol. Syst.* **46**, 215–235 https://doi.org/10.1146/annurev-ecolsys-110512-135808

6   Kump, L.R. (2008) The rise of atmospheric oxygen. *Nature* **451**, 277–278 https://doi.org/10.1038/nature06587

7   Kaltenegger, L., Traub, W.A. and Jucks, K.W. (2007) Spectral evolution of an Earth-like planet. *Astrophys. J.* **658**, 598–616 https://doi.org/10.1086/510996

8   Reinhard, C.T., Olson, S.L., Schwieterman, E.W. and Lyons, T.W. (2017) False negatives for remote life detection on ocean-bearing planets: lessons from the early earth. *Astrobiology* **17**, 287–297 https://doi.org/10.1089/ast.2016.1598

9   Lovelock, J.E. (1965) A physical basis for life detection experiments. *Nature* **207**, 568–570 https://doi.org/10.1038/207568a0

10   Hofmann, H.J., Grey, K., Hickman, A.H. and Thorpe, R.I. (1999) Origin of 3.45 Ga coniform stromatolites in Warrawoona Group, Western Australia. *Geol. Soc. Am. Bull.* **111**, 1256–1262 https://doi.org/10.1130/0016-7606(1999)111<1256:OOGCSI>2.3.CO;2

11   Farquhar, J., Bao, H. and Thiemens, M. (2000) Atmospheric influence of Earth's earliest sulfur cycle. *Science* **289**, 756–758 https://doi.org/10.1126/science.289.5480.756

12   Johnston, D.T. (2011) Multiple sulfur isotopes and the evolution of Earth's surface sulfur cycle. *Earth-Sci. Rev.* **106**, 161–183 https://doi.org/10.1016/j.earscirev.2011.02.003

13   Pavlov, A.A. and Kasting, J.F. (2002) Mass-independent fractionation of sulfur isotopes in Archean sediments: strong evidence for an anoxic Archean atmosphere. *Astrobiology* **2**, 27–41 https://doi.org/10.1089/153110702753621321

14   Bowman, D.M.J.S., Balch, J.K., Artaxo, P., Bond, W.J., Carlson, J.M., Cochrane, M.A. et al. (2009) Fire in the Earth system. *Science* **324**, 481–484 https://doi.org/10.1126/science.1163886

15   Scott, A.C. (2000) The pre-quaternary history of fire. *Palaeogeogr., Palaeoclimatol., Palaeoecol.* **164**, 281–329 https://doi.org/10.1016/S0031-0182(00)00192-9

16   Belcher, C.M. and McElwain, J.C. (2008) Limits for combustion in low O_2 redefine paleoatmospheric predictions for the Mesozoic (vol 321, pg 1197, 2008). *Science* **322**, 192 https://doi.org/10.1126/science.1160978

17   Canfield, D.E. (1998) A new model for Proterozoic ocean chemistry. *Nature* **396**, 450–453 https://doi.org/10.1038/24839

18   Yang, W.B. and Holland, H.D. (2003) The Hekpoort paleosol profile in Strata 1 at Gaborone, Botswana: Soil formation during the great oxidation event. *Am. J. Sci.* **303**, 187–220 https://doi.org/10.2475/ajs.303.3.187

19   Zbinden, E.A., Holland, H.D., Feakes, C.R. and Dobos, S.K. (1988) The sturgeon falls paleosol and the composition of the atmosphere 1.1 Ga Bp. *Precambrian Res.* **42**, 141–163 https://doi.org/10.1016/0301-9268(88)90014-9

20   Sheldon, N.D. (2006) Precambrian paleosols and atmospheric CO_2 levels. *Precambrian Res.* **147**, 148–155 https://doi.org/10.1016/j.precamres.2006.02.004

21   Sheldon, N.D. and Tabor, N.J. (2009) Quantitative paleoenvironmental and paleoclimatic reconstruction using paleosols. *Earth-Sci. Rev.* **95**, 1–52 https://doi.org/10.1016/j.earscirev.2009.03.004

22   Sheldon, N.D. and Retallack, G.J. (2001) Equation for compaction of paleosols due to burial. *Geology* **29**, 247–250 https://doi.org/10.1130/0091-7613(2001)029<0247:EFCOPD>2.0.CO;2

23   Mitchell, R.L. and Sheldon, N.D. (2009) Weathering and paleosol formation in the 1.1 Ga Keweenawan Rift. *Precambrian Res.* **168**, 271–283 https://doi.org/10.1016/j.precamres.2008.09.013

24   Mitchell, R.L. and Sheldon, N.D. (2010) The ~1100 Ma Sturgeon Falls paleosol revisited: Implications for Mesoproterozoic weathering environments and atmospheric CO_2 levels. *Precambrian Res.* **183**, 738–748 https://doi.org/10.1016/j.precamres.2010.09.003

25   Mitchell, R.L. and Sheldon, N.D. (2016) Sedimentary provenance and weathering processes in the 1.1 Ga Midcontinental Rift of the Keweenaw Peninsula, Michigan, USA. *Precambrian Res.* **275**, 225–240 https://doi.org/10.1016/j.precamres.2016.01.017

26   Cole, D.B., Reinhard, C.T., Wang, X., Gueguen, B., Halverson, G.P., Gibson, T. et al. (2016) A shale-hosted Cr isotope record of low atmospheric oxygen during the Proterozoic. *Geology* **44**, 555–558 https://doi.org/10.1130/G37787.1

27   Crowe, S.A., Døssing, L.N., Beukes, N.J., Bau, M., Kruger, S.J., Frei, R. et al. (2013) Atmospheric oxygenation three billion years ago. *Nature* **501**, 535–538 https://doi.org/10.1038/nature12426

28   Frei, R., Gaucher, C., Poulton, S.W. and Canfield, D.E. (2009) Fluctuations in Precambrian atmospheric oxygenation recorded by chromium isotopes. *Nature* **461**, 250–253 https://doi.org/10.1038/nature08266

29   Gilleaudeau, G.J., Frei, R., Kaufman, A.J., Kah, L.C., Azmy, K., Bartley, J.K. et al. (2016) Oxygenation of the mid-Proterozoic atmosphere: clues from chromium isotopes in carbonates. *Geochem. Perspect. Lett.* **2**, 178–187 https://doi.org/10.7185/geochemlet.1618

30   Fendorf, S., Wielinga, B.W. and Hansel, C.M. (2000) Chromium transformations in natural environments: the role of biological and abiological processes in chromium(VI) reduction. *Int. Geol. Rev.* **42**, 691–701 https://doi.org/10.1080/00206810009465107

31   Gueguen, B., Reinhard, C.T., Algeo, T.J., Peterson, L.C., Nielsen, S.G., Wang, X. et al. (2016) The chromium isotope composition of reducing and oxic marine sediments. *Geochim. Cosmochim. Acta* **184**, 1–19 https://doi.org/10.1016/j.gca.2016.04.004

32   Hood, A.V.s., Planavsky, N.J., Wallace, M.W. and Wang, X. (2018) The effects of diagenesis on geochemical paleoredox proxies in sedimentary carbonates. *Geochimica et Cosmochimica Acta* **232**, 265–287 https://doi.org/10.1016/j.gca.2018.04.022

33   Rodler, A., Sánchez-Pastor, N., Fernández-Díaz, L. and Frei, R. (2015) Fractionation behavior of chromium isotopes during coprecipitation with calcium carbonate: Implications for their use as paleoclimatic proxy. *Geochim. Cosmochim. Acta* **164**, 221–235 https://doi.org/10.1016/j.gca.2015.05.021

34   Learman, D.R., Voelker, B.M., Vazquez-Rodriguez, A.I. and Hansel, C.M. (2011) Formation of manganese oxides by bacterially generated superoxide. *Nat. Geosci.* **4**, 95–98 https://doi.org/10.1038/ngeo1055

35   Wang, X.L., Planavsky, N.J., Reinhard, C.T., Zou, H., Ague, J.J., Wu, Y. et al. (2016) Chromium isotope fractionation during subduction-related metamorphism, black shale weathering, and hydrothermal alteration. *Chem. Geol.* **423**, 19–33 https://doi.org/10.1016/j.chemgeo.2016.01.003

36   Oze, C., Sleep, N.H., Coleman, R.G. and Fendorf, S. (2016) Anoxic oxidation of chromium. *Geology* **44**, 543–546 https://doi.org/10.1130/G37844.1

37   Saad, E., Wang, X., Planavsky, N.J., Reinhard, C.T. and Tang, Y. (2018) Chromium isotope fractionation induced by ligand-promoted mobilization of a Cr (III)-containing mineral. *Nat. Commun.* **1590** https://doi.org/10.1038/s41467-017-01694-y

38   Thiemens, M.H. and Heidenreich, J.E. (1983) The mass-independent fractionation of oxygen: a novel isotope effect and its possible cosmochemical implications. *Science* **219**, 1073–1075 https://doi.org/10.1126/science.219.4588.1073

39   Thiemens, M.H. (2006) History and applications of mass-independent isotope effects. *Annu. Rev. Earth Planet. Sci.* **34**, 217–262 https://doi.org/10.1146/annurev.earth.34.031405.125026

40   Wen, J. and Thiemens, M.H. (1993) Multi-isotope study of the $O(^1D)$+CO_2 exchange and stratospheric consequences. *J. Geophys. Res.* **98**, 12801–12808 https://doi.org/10.1029/93JD00565

41   Segura, A., Krelove , K., Kasting, J.F., Sommerlatt, D., Meadows, V., Crisp, D. et al. (2003) Ozone concentrations and ultraviolet fluxes on Earth-like planets around other stars. *Astrobiology* **3**, 689–708 https://doi.org/10.1089/153110703322736024

42   Luz, B., Barkan, E., Bender, M.L., Thiemens, M.H. and Boering, K.A. (1999) Triple-isotope composition of atmospheric oxygen as a tracer of biosphere productivity. *Nature* **400**, 547–550 https://doi.org/10.1038/22987

43   Bao, H.M., Thiemens, M.H., Farquhar, J., Campbell, D.A., Lee, C.C.-W., Heine, K. et al. (2000) Anomalous ^{17}O compositions in massive sulphate deposits on the Earth. *Nature* **406**, 176–178 https://doi.org/10.1038/35018052

44   Cao, X.B. and Bao, H.M. (2013) Dynamic model constraints on oxygen-17 depletion in atmospheric O_2 after a snowball Earth. *Proc. Natl Acad. Sci. U.S.A.* **110**, 14546–14550 https://doi.org/10.1073/pnas.1302972110

45   Crockford, P., Hayles, J., Bao, H., Planavsky, N.J., Bekker, A., Frallick, P.W. et al. Limited primary production sustained low mid-Proterozoic oxygen levels. *Nature*, **559**, 613–616 https://doi.org/10.1038/s41586-018-0349-y

46   Pack, A., Höweling, A., Hezel, D.C., Stefanak, M.T., Beck, A.-K., Peters, S.T.M. et al. (2017) Tracing the oxygen isotope composition of the upper Earth's atmosphere using cosmic spherules. *Nat. Commun.* **8**, 15702 https://doi.org/10.1038/ncomms15702

47   Laakso, T.A. and Schrag, D.P. (2017) A theory of atmospheric oxygen. *Geobiology* **15**, 366–384 https://doi.org/10.1111/gbi.12230

48   Laakso, T.A. and Schrag, D.P. (2014) Regulation of atmospheric oxygen during the Proterozoic. *Earth Planet. Sci. Lett.* **388**, 81–91 https://doi.org/10.1016/j.epsl.2013.11.049

49   Katsev, S. and Crowe, S.A. (2015) Organic carbon burial efficiencies in sediments: The power law of mineralization revisited. *Geology* **43**, 607–610 https://doi.org/10.1130/G36626.1

50   Zhao, M.Y., Reinhard, C.T. and Planavsky, N. (2018) Terrestrial methane fluxes and Proterozoic climate. *Geology* **46**, 139–142 https://doi.org/10.1130/G39502.1

51   Kunzmann, M., Bui, T.H., Crockford, P.W., Halverson, G.P., Scott, C., Lyons, T.W. et al. (2017) Bacterial sulfur disproportionation constrains timing of Neoproterozoic oxygenation. *Geology* **45**, 207–210 https://doi.org/10.1130/G38602.1

52   Liu, X.-M., Kah, L.C., Knoll, A.H., Cui, H., Kaufman, A.J., Shahar, A. et al. (2016) Tracing Earth's O_2 evolution using Zn/Fe ratios in marine carbonates. *Geochem. Perspect. Lett.* **2**, 24–34 https://doi.org/10.7185/geochemlet.1603

53   Zhang, S., Wang, X., Wang, H., Bjerrum, C., Hammarlund, E.U., Costa, M.M. et al. (2016) Sufficient oxygen for animal respiration 1,400 million years ago. *Proc. Natl Acad. Sci. U.S.A.* **113**, 1731–1736 https://doi.org/10.1073/pnas.1523449113

54   Daines, S.J., Mills, B.J.W. and Lenton, T.M. (2017) Atmospheric oxygen regulation at low Proterozoic levels by incomplete oxidative weathering of sedimentary organic carbon. *Nat. Commun.* **8**, 14379 https://doi.org/10.1038/ncomms14379

55   Canfield, D.E., Poulton, S.W., Knoll, A.H., Narbonne, G.M., Ross, G., Goldberg, T. et al. (2008) Ferruginous conditions dominated later Neoproterozoic deep-water chemistry. *Science* **321**, 949–952 https://doi.org/10.1126/science.1154499

56   Dahl, T.W., Canfield, D.E., Rosing, M.T., Frei, R.E., Gordon, G.W., Knoll, A.H. et al. (2011) Molybdenum evidence for expansive sulfidic water masses in ~750 Ma oceans. *Earth Planet. Sci. Lett.* **311**, 264–274 https://doi.org/10.1016/j.epsl.2011.09.016

57   Sperling, E.A., Wolock, C.J., Morgan, A.S., Gill, B.C., Kunzmann, M., Halverson, G.P. et al. (2015) Statistical analysis of iron geochemical data suggests limited late Proterozoic oxygenation. *Nature* **523**, 451–454 https://doi.org/10.1038/nature14589

58   Wallace, M.W., Hood, A.S., Shuster, A., Greig, A., Planavsky, N.J. and Reed, C.P. (2017) Oxygenation history of the Neoproterozoic to early Phanerozoic and the rise of land plants. *Earth Planet. Sci. Lett.* **466**, 12–19 https://doi.org/10.1016/j.epsl.2017.02.046

59   Poulton, S.W. and Canfield, D.E. (2011) Ferruginous conditions: a dominant feature of the ocean through Earth's history. *Elements* **7**, 107–112 https://doi.org/10.2113/gselements.7.2.107

60   Petrash, D.A., Gueneli, N., Brocks, J.J., Mendez-Dot, J.A., Gonzalez-Arismendi, G., Poulton, S.W. et al. (2016) Black shale deposition and early diagenetic dolomite cementation during oceanic anoxic event 1: the mid-Cretaceous Maracaibo platform, northwestern South America. *Am. J. Sci.* **316**, 669–711 https://doi.org/10.2475/07.2016.03

61   Slack, J.F., Grenne, T. and Bekker, A. (2009) Seafloor-hydrothermal Si-Fe-Mn exhalites in the Pecos greenstone belt, New Mexico, and the redox state of ca. 1720 Ma deep seawater. *Geosphere* **5**, 302–314 https://doi.org/10.1130/GES00220.1

62   Sperling, E.A., Rooney, A.D., Hays, L., Sergeev, V.N., Vorob'eva, N.G., Sergeeva, N.D. et al. (2014) Redox heterogeneity of subsurface waters in the Mesoproterozoic ocean. *Geobiology* **12**, 373–386 https://doi.org/10.1111/gbi.12091

63   Reinhard, C.T., Planavsky, N.J., Olson, S.L., Lyons, T.W. and Erwin, D.H. (2016) Earth's oxygen cycle and the evolution of animal life. *Proc. Natl Acad. Sci. U.S.A.* **113**, 8933–8938 https://doi.org/10.1073/pnas.1521544113

64   Derry, L.A. (2015) Causes and consequences of mid-Proterozoic anoxia. *Geophys. Res. Lett.* **42**, 8538–8546 https://doi.org/10.1002/2015GL065333

65   Reinhard, C.T., Planavsky, N.J., Gill, B.C., Ozaki, K., Robbins, L.J., Lyons, T.W. et al. (2017) Evolution of the global phosphorus cycle. *Nature* **541**, 386–389 https://doi.org/10.1038/nature20772

66   Bjerrum, C.J. and Canfield, D.E. (2002) Ocean productivity before about 1.9 Gyr ago limited by phosphorus adsorption onto iron oxides. *Nature* **417**, 159–162 https://doi.org/10.1038/417159a

67   VanCappellen, P. and Ingall, E.D. (1996) Redox stabilization of the atmosphere and oceans by phosphorus-limited marine productivity. *Science* **271**,
        493–496 https://doi.org/10.1126/science.271.5248.493

68   Pinto, J.P. and H. H. (1988) Paleosols and the evolution of the atmosphere: Part II. In *Paleosols and Weathering Through Geologic Time: Principles and
        Applications* (Reinhardt, J. and S. W., eds), pp. 21–34, GSA, Denver

69   Kump, L.R. (2014) Hypothesized link between Neoproterozoic greening of the land surface and the establishment of an oxygen-rich atmosphere. *Proc.
        Natl Acad. Sci. U.S.A.* **111**, 14062–14065 https://doi.org/10.1073/pnas.1321496111

70   Sheldon, N.D. (2013) Causes and consequences of low atmospheric pCO$_2$ in the Late Mesoproterozoic. *Chem. Geol.* **362**, 224–231 https://doi.org/10.
        1016/j.chemgeo.2013.09.006

71   Liivamagi, S. et al. (2015) Petrology, mineralogy and geochemical climofunctions of the Neoproterozoic Baltic paleosol. *Precambrian Research* **256**,
        170–188

72   Sheldon, N.D. (2003) Pedogenesis and geochemical alteration of the Picture Gorge subgroup, Columbia River Basalt, Oregon. *Geological Society of
        America Bulletin* **115**, 1377–1387

73   Bach, L.T., Riebesell, U., Sett, S., Febiri, S., Rzepka, P. and Schulz, K.G. (2012) An approach for particle sinking velocity measurements in the 3–400
        μm size range and considerations on the effect of temperature on sinking rates. *Mar. Biol.* **159**, 1853–1864 https://doi.org/10.1007/
        s00227-012-1945-2

74   Thullner, M., Dale, A.W. and Regnier, P. (2009) Global-scale quantification of mineralization pathways in marine sediments: A reaction-transport
        modeling approach. *Geochem., Geophys., Geosyst.* **10**, Q10012 https://doi.org/10.1029/2009GC002484

75   Woodward, F. (2007) Global primary production. *Curr. Biol.* **17**, R269–R273 https://doi.org/10.1016/j.cub.2007.01.054